The *sup-pf-2* Mutations of *Chlamydomonas* Alter the Activity of the Outer Dynein Arms by Modification of the γ-Dynein Heavy Chain

Gerald Rupp,* Eileen O'Toole,‡ Lynne C. Gardner,* Beth F. Mitchell,§ and Mary E. Porter*

*Department of Cell Biology and Neuroanatomy, University of Minnesota Medical School, Minneapolis, Minnesota 55455; ‡Department of Molecular, Cellular, and Developmental Biology, University of Colorado at Boulder, Boulder, Colorado 80309-0347; and §Department of Biology, LeMoyne College, Syracuse, New York 13214

Abstract. The *sup-pf-2* mutation is a member of a group of dynein regulatory mutations that are capable of restoring motility to paralyzed central pair or radial spoke defective strains. Previous work has shown that the flagellar beat frequency is reduced in *sup-pf-2*, but little else was known about the *sup-pf-2* phenotype (Huang, B., Z. Ramanis, and D.J.L. Luck. 1982. *Cell.* 28:115–125; Brokaw, C.J., and D.J.L. Luck. 1985. *Cell Motil.* 5:195–208). We have reexamined *sup-pf-2* using improved biochemical and structural techniques and by the analysis of additional *sup-pf-2* alleles. We have found that the *sup-pf-2* mutations are associated with defects in the outer dynein arms. Biochemical analysis of *sup-pf-2-1* axonemes indicates that both axonemal ATPase activity and outer arm polypeptides are reduced by 40–50% when compared with wild type. By thin-section EM, these defects correlate with an ~45% loss of outer dynein arm structures. Interestingly, this loss is biased toward a subset of outer doublets, resulting in a radial asymmetry that may reflect some aspect of outer arm assembly. The defects in outer arm assembly do not appear to result from defects in either the outer doublet microtubules or the outer arm docking structures, but rather appear to result from defects in outer dynein arm components. Analysis of new *sup-pf-2* mutations indicates that the severity of the outer arm assembly defects varies with different alleles. Complementation tests and linkage analysis reveal that the *sup-pf-2* mutations are alleles of the *PF28/ODA2* locus, which is thought to encode the γ-dynein heavy chain subunit of the outer arm. The *sup-pf-2* mutations therefore appear to alter the activity of the outer dynein arms by modification of the γ-dynein heavy chain.

THE dynein ATPases provide the driving force for ciliary and flagellar motility and participate in numerous aspects of microtubule-based transport. In the axoneme, these large, multisubunit enzymes form the inner and outer arm structures that are bound to the outer doublet microtubules and interact transiently with adjacent doublet microtubules to generate the force for interdoublet sliding (for reviews see Mitchell, 1994; Porter, 1996). In *Chlamydomonas*, both the outer and inner dynein arms have been extensively characterized. The outer arms contain three dynein heavy chains (DHCs;[1] >400 kD, referred to as α, β, and γ), two intermediate chains (ICs; 69 and 78 kD), and eight light chains (LCs; 8–20 kD), and they are bound to the outer doublets every 24 nm along the length of the axoneme (see Witman et al., 1994). The inner dynein arms are much more diverse; seven different molecular complexes (one two-headed, and six single-headed isoforms) have been identified (Kagami and Kamiya, 1992). The isolated inner arm complexes appear to be structurally and biochemically similar to the outer arms (Goodenough et al., 1987), but they may be asymmetrically distributed along the length of the axoneme (Piperno et al., 1990; Piperno and Ramanis, 1991; Gardner et al., 1994). Despite their similarities, the inner and outer dynein arms appear to have different functions in the generation of flagellar motility. The inner arms are both necessary and sufficient to initiate interdoublet sliding and propagate bends, whereas the outer arms increase sliding velocity and add power to the flagellar beat (Brokaw and Kamiya, 1987). Functional diversity has also been observed among individual DHCs. For instance, analysis of different outer arm mutations indicates that the absence of a functional β-DHC causes a more serious motility de-

Address all correspondence to Mary E. Porter, Department of Cell Biology and Neuroanatomy, University of Minnesota Medical School, 4-135 Jackson Hall, 321 Church St., Minneapolis, MN 55455. Tel.: (612) 626-1901. Fax: (612) 624-8118. e-mail: mary-p@biosci.cbs.umn.edu

1. *Abbreviations used in this paper*: cM, centimorgans; CP, central pair; DHC, dynein heavy chain; FPLC, fast protein liquid chromatography; HSE, dynein-containing high salt extract; IC, intermediate chain; LC, light chain; RS, radial spoke.

fect than the absence of the α-DHC (Sakakibara et al., 1991, 1993). Since the β-DHC accounts for most of the ATPase activity of the αβ complex (Pfister and Witman, 1984), it has been postulated that the β-DHC is responsible for force production, whereas the α-DHC and possibly the γ-DHC act as amplifiers or modulators of β-DHC activity (Sakakibara et al., 1993). Other studies have indicated that the different inner arm isoforms also have different functions in the formation of flagellar waveform (Kagami and Kamiya, 1992; Minoura and Kamiya, 1995).

Since dynein arms can generate sliding forces in only one direction (Sale and Satir, 1977; Fox and Sale, 1987), the activity of the multiple dynein isoforms must be coordinated both spatially and temporally to generate an efficient flagellar waveform. If all the dynein arms were active simultaneously, no net motion would occur. Both structural and genetic evidence have implicated the central pair (CP) and radial spoke (RS) structures as key regulators of dynein arm activity. The orientation of the radial spokes changes when local bending occurs (Warner and Satir, 1974), and, in some species, including *Chlamydomonas*, the central pair rotates once per beat cycle (Omoto and Kung, 1979; Omoto and Witman, 1981; Kamiya, 1982). Moreover, mutations that disrupt either the CP or RS structures result in flagellar paralysis (Witman et al., 1978) by a mechanism that appears to involve global inactivation of dynein arm activity (Huang et al., 1982; Smith and Sale, 1992*a*). One hypothesis is that the central pair projections periodically sweep the radial spoke heads like a distributor, inducing a local signal that is transmitted to the dynein arms (Omoto and Kung, 1979). In the absence of these signals, other axonemal components must inhibit dynein activity in CP or RS mutant cells.

New insights into the nature of this inhibitory control system recently have been obtained by the characterization of extragenic suppressor mutations that restore motility to CP/RS defective strains without restoring the missing CP or RS structures. Second-site mutations in eight different loci (*sup-pf-1*, *sup-pf-2*, *sup-pf-3*, *sup-pf-4*, *sup-pf-5*, *pf2*, *pf3*, *pf9-2*) short-circuit the inhibitory control system and allow for some dynein arm activity in the absence of signals from the CP/RS complex (Huang et al., 1982; Piperno et al., 1992; Porter at al., 1992). These suppressors are thought to identify components in the signaling pathway between the radial spokes and the dynein arms. Recent studies have suggested that there are at least three different classes of suppressors: one class that identifies regulatory domains located within the outer dynein arm (*sup-pf-1*; Huang et al., 1982; Porter et al., 1994), a second class that alters the assembly of an inner dynein arm isoform (*pf9-2*; Porter et al., 1992), and a third class that alters components of a dynein regulatory complex as well as the assembly of a subset of the inner dynein arms (*sup-pf-3*, *sup-pf-4*, *sup-pf-5*, *pf2*, *pf3*), which are located in close proximity to the dynein regulatory complex (Huang et al., 1982; Piperno et al., 1992; Gardner et al., 1994; Piperno et al., 1994).

The *sup-pf-2* mutation was recovered in the original collection of suppressor strains (Huang et al., 1982), but it has not been well characterized. Early studies have identified defects in *sup-pf-2* motility, i.e., a reduced beat frequency (Brokaw and Luck, 1985), but no biochemical or structural defects were previously described (Huang et al., 1982). Given recent improvements in structural techniques (Mastronarde et al., 1992) and in the resolution of dynein heavy chain polypeptides (Kagami and Kamiya, 1992), we decided to reexamine the *sup-pf-2* strain for possible defects in inner arm components. Much to our surprise, we have discovered that the defects in *sup-pf-2* are associated with the outer dynein arms. In addition, we have found that the *sup-pf-2* mutations are alleles of the *PF28/ODA2* locus, which has been reported to encode the outer arm γ-DHC (Wilkerson et al., 1994). These results provide new insights into the genes and gene products involved in regulation of dynein arm activity and the assembly of outer arm components.

Materials and Methods

Strains and Cell Culture

Characteristics of the outer arm mutant strains used in this study are listed in Table I. Additional strains used were *arg2*, *arg7*, *pf1*, *pf14*, *ery1b*, and 137c (wild type). Cells were maintained as vegetatively growing cultures at 21°C on rich medium containing sodium acetate, as described by Sager and Granick (1953) and modified by Holmes and Dutcher (1989). *arg* strains were maintained on rich medium supplemented with 2.85 mM L-arginine. Progeny from crosses involving *ery1b* were scored for drug resistance on rich medium and rich medium supplemented with 200 μg/ml erythromycin. Cultures of gametic cells were obtained by transferring strains to a low sulfate medium for 5–7 d. All solid media contained Bacto agar (Difco Laboratories, Detroit, MI) washed with deionized water and air dried before use. Media for large scale (>5 liters) liquid cultures were supplemented with additional phosphate as described by Witman (1986).

Genetic Analysis

Complementation tests were performed by constructing stable diploid cell lines (Ebersold, 1967). Each mutation was crossed into an appropriate arginine-requiring background (either *arg2* or *arg7*), and diploids were selected on medium lacking arginine. Six or more independently isolated cell lines were examined for each diploid construct, and all diploids were demonstrated to be mating type minus. Complementation tests were not performed with *oda4* alleles because previous work has shown that the *oda4* and *sup-pf-1* mutations are alleles at the same locus (Porter et al., 1994) and that the *sup-pf-1* and *sup-pf-2* mutations are unlinked (Huang et al., 1982; Mitchell, B., manuscript in preparation).

Genetic mapping was accomplished by recombination analysis of tetrad

Table I. Characteristics of Outer Arm Mutants Used in This Study

Strain	Axonemal defect	Defective gene product	References*
oda1-99	Outer arms and outer doublet projections missing		1,2
oda2 (pf28)	Outer arms missing	γ-DHC	1,3,4
oda3	Outer arms and outer doublet projections missing		1,2
oda5	Outer arms missing		1
oda6-95	Outer arms missing	IC69	1,5
oda7	Outer arms missing		1
oda8	Outer arms missing		1
oda9	Outer arms missing	IC78	1,4
oda10	Outer arms missing		1
oda11	α-DHC/LC missing	α-DHC	6
sup-pf-2	Unknown		7

*1: Kamiya, 1988; 2: Takada and Kamiya, 1994; 3: Mitchell and Rosenbaum, 1985; 4: Wilkerson et al., 1994; 5: Mitchell and Kang, 1991; 6: Sakakibara et al, 1991; 7: Huang et al., 1982.

progeny using standard techniques (Levine and Ebersold, 1960). The cross of *sup-pf-2* to *arg2* resulted in a 10:3:5 (parental ditype [PD]/nonparental ditype [NPD]/tetratype [TT]) segregation of tetrad progeny. The large number of recombinant tetrads indicates that these two mutations are unlinked and further suggests that the original assignment of *sup-pf-2* to linkage group I was incorrect (Huang et al., 1982).

Motility Measurements

Swimming behavior was observed by phase-contrast microscopy on a microscope (Axioskop; Carl Zeiss, Inc., Thornwodd, NY) using a ×40 objective and low intensity illumination. Measurements of swimming velocities were made from video recordings (BC-1000 VCR; Mitsubishi Electric Sales of America, Cypress, CA) of live cells using a camera (C2400 Newvicon; Hamamatsu Photonic Systems Corp., Bridgewater, NJ) and a video processor (Argus 10; Hamamatsu Photonic Systems Corp.) calibrated with a stage micrometer. Beat frequency was measured stroboscopically using dark-field illumination.

Protein Purification

Whole axonemes were obtained from small scale cultures of gametic cells on solid medium. The cells were resuspended in minimal medium, allowed to generate flagella for 45–60 min, and collected by centrifugation. Cells were washed free of debris and cell wall material by two cycles of resuspension and centrifugation in minimal medium, resuspended in 10 mM Hepes, pH 7.4, 1 mM $SrCl_2$, 4% sucrose, and 1 mM DTT, and then deflagellated by pH shock (Witman et al., 1972). The solution of deflagellated cells was then supplemented to 5 mM $MgSO_4$, 1 mM EGTA, 0.1 mM EDTA, and 5 μg/ml aprotinin, leupeptin, and pepstatin and centrifuged at 1,000 *g* at 4°C. The flagella-containing supernatant was recentrifuged twice over a 20% sucrose cushion to remove remaining cell bodies and debris. The clarified flagella were extracted with 0.1% NP-40, and the axonemes were collected by centrifugation at 35,000 *g* for 60 min. The axoneme pellet was then resuspended in HMEEN buffer (30 mM Hepes, pH 7.4, 5 mM $MgSO_4$, 1 mM EGTA, 0.1 mM EDTA, 25 mM NaCl, 1 mM DTT, and 5 μg/ml aprotinin, leupeptin, and pepstatin), split into two aliquots, and recentrifuged at 14,000 *g* to obtain parallel samples for gel electrophoresis and EM.

Purified dyneins were prepared from large scale cultures (20–40 liters) of vegetative cells. Cells were collected using a Pellicon Cell Harvester (Millipore Corp., Bedford, MA) equipped with Durapore filter cassettes. Concentrated cells were washed and deflagellated as described above. The final supernatant of clarified flagella was collected directly by centrifugation, resuspended in HMEEN, extracted with 1% NP-40, washed two to three times to remove the detergent, and then extracted in HMEEN containing 0.6 M NaCl, 0.1 mM ATP, and 10 μM taxol for 30 min on ice. The dynein-containing supernatant was collected after centrifugation at 30,000 *g* for 30 min and immediately prepared for fractionation by fast protein liquid chromatography (FPLC) or sucrose density gradient centrifugation.

Ion Exchange Chromatography

Separation of dynein extracts by ion exchange chromatography was performed as described by Goodenough et al. (1987) with modifications by Kagami and Kamiya (1992) and Gardner et al. (1994). All procedures for dynein fractionation were carried out at 4°C. Chromatography was performed at a flow rate of 1.5 ml/min on an analytical anion exchange column (Mono-Q HR5/5; Pharmacia Biotech, Inc., Piscataway, NJ). The dynein-containing extract (0.5–1 mg total protein) was diluted in 9 vol of chromatography buffer (20 mM Hepes, pH 7.4, 10 mM NaCl, 5 mM $MgSO_4$, 1 mM DTT, and 1 μg/ml leupeptin) and immediately loaded onto an equilibrated column. The column was briefly washed with buffer containing 100 mM NaCl, and then eluted with a linear 100–400 mM NaCl gradient applied over 40 ml. Fractions of 0.5 ml were collected and analyzed by SDS-PAGE.

Sucrose Density Gradient Centrifugation

High salt extracts containing crude dynein were dialyzed against HMEEN supplemented with 0.1 mM DTT and 2.5 μg/ml aprotinin, leupeptin, and pepstatin for 6–24 h at 4°C, centrifuged at 39,000 *g* for 30 min, and loaded onto a 13-ml 5–20% sucrose gradient. The gradients were centrifuged in a swinging bucket rotor (SW41; Beckman Instruments, Inc., Palo Alto, CA) at 33,700 rpm for 14 h at 4°C. After centrifugation, 0.6-ml fractions were collected and analyzed by ATPase activity and SDS-PAGE.

Dynein Rebinding Experiments

Axonemes from large scale cultures of wild-type and *sup-pf-2* cells were prepared as described above, assayed for protein concentration, and brought to 10 mg/ml. The *sup-pf-2* sample and a portion of the wild-type sample were stored on ice for later use. The remaining wild-type sample was pelleted and resuspended in an equal volume of high salt solution (HMEEN made to 0.6 M NaCl and supplemented with 0.1 mM ATP, 10 μM taxol) and extracted for 30 min on ice. The axonemes were pelleted by centrifugation (15,000 *g*, 30 min, 4°C), and the supernatant was dialyzed against HMEEN supplemented with 0.1 mM DTT and 2.5 μg/ml aprotinin, leupeptin, and pepstatin for 2 h at 4°C. This crude dynein-containing high salt extract (HSE) was supplemented to a final concentration of 0.5 mM ATP and 100 μM vanadate to inhibit binding by the ATP-sensitive sites, and then recombined with unextracted wild-type and *sup-pf-2* axonemes at stoichiometric ratios of 0:1, 0.5:1, 1:1, and 2:1, essentially as described by Smith and Sale (1992*b*). The extract/axoneme mixtures were incubated at room temperature for 15–20 min, after which the axonemes were pelleted at 16,000 *g* for 20 min. Supernatants were collected, axoneme pellets were resuspended in an appropriate volume, and samples were prepared for SDS-PAGE and EM as described below.

Biochemical Analyses

The ATPase activity of whole axonemes, extracted outer doublets, high salt extracts, and sucrose gradient fractions was measured in the presence of 300 mM KCl, 30 mM Tris, pH 8.0, 5 mM $MgSO_4$, 0.1 mM EGTA, and 1 mM ATP. Under these conditions, dynein ATPase activity is presumed to be uncoupled from axonemal motility. Inorganic phosphate released was determined colorimetrically by the method of Waxman and Goldberg (1982). High salt extraction routinely solubilized >85% of the axonemal ATPase activity. Protein concentrations were determined by the method of Bradford (1976) using BSA as a standard.

The dynein heavy chains were resolved by SDS-PAGE using 3–5% polyacrylamide, 3–8 M urea gradient gels (Kagami and Kamiya, 1990) using the buffer system of Laemmli (1970). Separations of other polypeptides were performed using either 5–15% polyacrylamide, 0–2.5 M glycerol gradient gels, 5–20% polyacrylamide, 0–2.5 M glycerol gradient gels, or 18% polyacrylamide gels. All gels were stained with silver (Wray et al., 1981), with the exception of the samples from the dynein rebinding experiments, which were stained with Coomassie blue for subsequent densitometric analysis (BioRad Scanning Densitometer; Bio Rad Laboratories, Richmond, CA).

EM and Image Analysis

Axonemes were prepared for EM as previously described (Porter et al., 1992). Briefly, axonemes were fixed with 2% glutaraldehyde and 4% tannic acid (Mallinkrodt Inc., St. Louis, MO) in 50 mM sodium phosphate, pH 6.9, for 1 h at room temperature, followed by fixation overnight in 2% glutaraldehyde in 50 mM sodium phosphate, pH 6.9, at 4°C. The samples were transferred to fresh fixative, postfixed in 1% OsO_4, dehydrated in a graded acetone series, and embedded in Epon-Araldite. Sections of 60-nm nominal thickness were stained with uranyl acetate and lead citrate and photographed for cross-sectional analysis. Images were obtained using either a Philips CM10 (Philips Electronic Instruments Co., Mahwah, NJ) or JEOL 100CX (JEOL USA, Inc., Peabody, MA) microscope operating at 80 kV.

The methods for digitizing, averaging, and comparing cross-sectional outer doublets were as previously described (Mastronarde et al., 1992), with the only modification being that the averages were normalized to the inner dynein arm using a program that scaled the background image intensity to zero, and the mean intensity of the region enclosing the inner arm to one.

Cross-sections of the proximal region of the axoneme were identified by the presence of morphological markers such as B-tubule projections in outer doublets 1, 5, and 6, and/or a two-membered crossbridge between outer doublets 1 and 2 (Hoops and Witman, 1983). Outer doublets from the proximal region of the axoneme were selected, oriented for doublet numbering, and scored for the presence or absence of the outer dynein arms or the small, pointed structure that is usually located at the outer arm binding site (Takada and Kamiya, 1994).

Isolation of New sup-pf-2 Alleles

Revertants of paralyzed *pf1* cells were induced by UV irradiation essentially as described by Luck et al. (1977). Cells were suspended to a concentration of 3.1×10^7 cells per ml, placed in 100-mm sterile petri dishes, and irradiated under a 40-W germicidal lamp (254 nm) for 6 min at a distance of 20 cm with stirring. Treated cells were placed in sterile tubes with 4 ml of medium I (Sager and Granick, 1953) and placed in the dark overnight before transfer to constant light. After 14 d, each tube was visually screened for evidence of swimming cells. Tubes containing motile revertants were numbered and plated onto solid media for single colony isolation. One representative colony from each tube was selected for further analysis. Each motile revertant displayed a similar swimming phenotype in which the flagella beat rapidly but the cells do not progress forward.

All new mutations were backcrossed to wild-type cells and tested for linkage with *pf1* by standard techniques (Levine and Ebersold, 1960). Extragenic pseudorevertants were first identified as bypass suppressors based on Western blot and genetic analyses, and then tested for allelism to known suppressor loci by linkage analysis. Suppressed (*sup*) *pf1* strains were crossed to a *sup-pf-1 pf1* double mutant and the tetrad progeny screened for paralyzed cells. Suppressed *pf1* strains producing paralyzed progeny from this cross were not allelic to *sup-pf-1*; these were therefore crossed to a *sup-pf-2-1 pf1* double mutant and again examined for paralyzed progeny. 11 new alleles of *sup-pf-2-1* were recovered in this screen (Mitchell, B., manuscript in preparation). Two of these suppressors (S3 and S14) were selected for further study in this report.

Results

Motility Defects

To determine whether *sup-pf-2* cells might have either an outer or inner arm dynein defect, we examined their motility phenotype in comparison with both wild-type and other mutant strains. Strains with outer dynein arm defects typically show reductions in swimming velocity, axonemal ATPase activity, and beat frequency (Mitchell and Rosenbaum, 1985; Brokaw and Kamiya, 1987; Kamiya, 1988), whereas strains with inner arm defects usually display reduced swimming velocities with near normal beat frequencies and ATPase activities (Brokaw and Kamiya, 1987; Kamiya et al., 1991; Porter et al., 1992). As shown in Table II, the swimming speed of *sup-pf-2* cells is reduced to ~50% of wild-type levels, while beat frequency is reduced by one third (Brokaw and Luck, 1985). These characteristics are intermediate between those observed with *oda11*, a mutant that lacks the outer arm α-DHC and its associated LC (Sakakibara et al., 1991), and those observed with *pf28*, a mutant that completely lacks outer arm structures (Mitchell and Rosenbaum, 1985). Similar results were observed when comparing axonemal ATPase activity (see Table II).

Dynein Isoforms in sup-pf-2 Axonemes

To characterize the nature of the dynein defect, axonemes were prepared from wild-type, *sup-pf-2*, *oda11*, and *pf28* strains, and their polypeptide compositions were compared by SDS-PAGE. Analysis of 3–5% polyacrylamide gradient gels indicates that each wild-type DHC is present in the *sup-pf-2* axonemes, but that some DHCs have a reduced staining intensity (Fig. 1). The bands of lowered staining intensity comigrate precisely with the α-, β-, and γ-DHCs of the outer dynein arms. To better resolve this apparent outer arm defect, isolated wild-type and *sup-pf-2* axonemes were salt extracted, and the dynein-containing supernatants were then fractionated either by sucrose density gradient centrifugation or by ion exchange chromatography on a Mono-Q column.

As shown in Fig. 2, stoichiometric amounts of wild-type and *sup-pf-2* dynein extracts were spun on 5–20% sucrose

Table II. Motility and ATPase Activity of Selected Strains

Strain	Beat frequency	Swimming velocity	Axonemal ATPase
	*Hz**	*μm/s*	*% of wt*
137c (wt)	63 ± 6.3	137 ± 15	100
oda2 (pf28)	22 ± 2	47.3 ± 6.8	20
oda11	52.6 ± 6.3	109 ± 14.8	80.7
sup-pf-2	40.2 ± 0.9	70.7 ± 9.8	52.6

Beat frequency and swimming velocity are expressed as mean ± SD ($n \geq 30$).
*Data from Brokaw and Luck, 1985; Mitchell and Rosenbaum, 1985; Sakakibara et al., 1991; Porter et al., 1994.

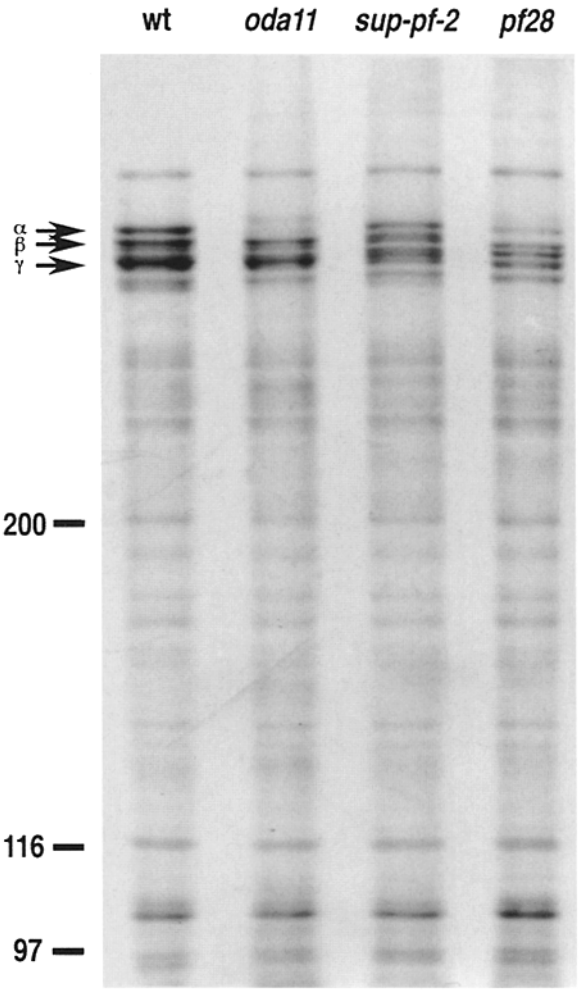

Figure 1. Dynein heavy chains in wild-type (*wt*), *oda11*, *sup-pf-2*, and *pf28* axonemes. The top portion of a silver-stained, 3–5% acrylamide, 3–8 M urea gradient gel is shown here. Whole axoneme samples like those depicted here contain DHCs contributed from both the inner and outer dynein arms. (*Arrows*) Location of the outer arm α-, β-, and γ-DHCs (intensely stained bands in *wt* lane). *oda11* is missing only the outer arm α-DHC band, while *pf28* is missing all three outer arm DHCs but contains a full complement of inner arm DHCs. Each lane was loaded with 2 μg of total axonemal protein (note the equivalent staining intensity of bands in the 97–200-kD range across the lanes). The positions of the molecular mass markers are indicated (*left*).

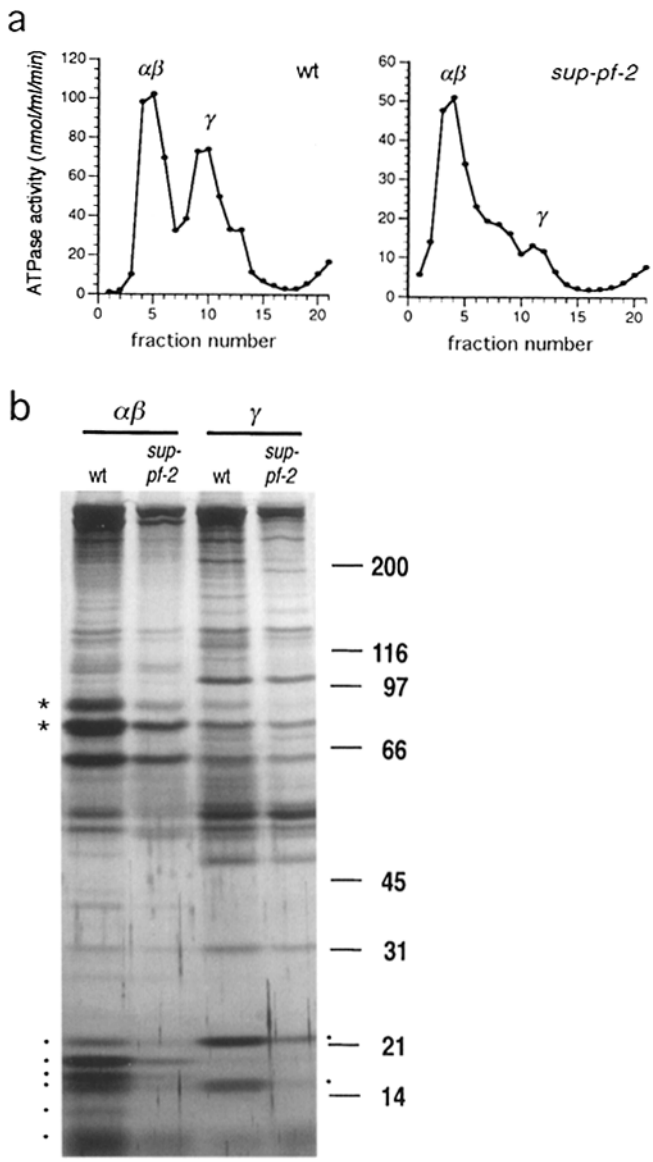

Figure 2. Fractionation of dynein extracts by sucrose density gradient centrifugation. (*a*) Stoichiometric amounts of wild-type and *sup-pf-2* dynein extracts were fractionated on 5–20% sucrose density gradients, and then assayed for ATPase activity. The 21S ($\alpha\beta$) and 12S (γ) peaks of ATPase activity are indicated in each profile. (*b*) SDS-PAGE pattern of the intermediate and light chains. Equal volumes of the 21S and 12S peak fractions were loaded onto a 5–15% acrylamide, 0–2.4 M glycerol gradient gel and stained with silver. The αβ-DHC–associated ICs (78 and 69 kD) and LCs (8–20 kD) are indicated on the left by asterisks and dots, respectively. The γ-DHC–associated LCs (18 and 22 kD) are indicated by dots on the right. The positions of the molecular mass markers are indicated (*right*).

density gradients, and then each fraction was assayed for ATPase activity to identify those fractions containing the outer arm dynein isoforms. Under these experimental conditions, wild-type outer dynein arms dissociate into two complexes: an αβ complex sedimenting at ~21S and a γ complex sedimenting at 12S (Piperno and Luck, 1979; Pfister and Witman, 1984). As shown in Fig. 2 *a*, the ATPase activity of the αβ peak in the *sup-pf-2* sample (52 nmol/ml/min) was about one half that of the wild-type αβ peak (105 nmol/ml/min), consistent with the decrease previously observed with whole axonemes (see Table II). Interestingly, the ATPase activity of the γ peak in the *sup-pf-2* sample (13 nmol/ml/min) was only 20% of that of the wild-type sample (74 nmol/ml/min). These results suggested that the primary defect might reside in either the outer arm γ complex (containing the γ-DHC and two LCs) or the cosedimenting inner arm isoforms. To determine if there were specific defects in the outer arm ICs or LCs, the αβ- and γ-DHC peak fractions from wild-type and *sup-pf-2* samples were further analyzed on 5–15% polyacrylamide gradient gels. As shown in Fig. 2 *b*, all the ICs and LCs associated with the wild-type αβ- and γ-DHC complexes were present in *sup-pf-2* fractions, albeit at reduced levels.

To better evaluate the inner arm dynein isoforms present, dynein extracts from wild-type and *sup-pf-2* axonemes were fractionated by FPLC ion exchange chromatography. This procedure identifies nine dynein complexes: one representing the outer arm αβ complex, one representing the outer arm γ complex, and seven others (*a–g*) corresponding to the inner arm dynein isoforms (for details, see Kagami and Kamiya, 1992, and Gardner et al., 1994). Fig. 3 *a* is an example of the FPLC profiles obtained with wild-type and *sup-pf-2* extracts. The outer arm dynein isoforms can be readily identified in the wild-type profile, where the γ subunit elutes near the beginning of the gradient, and the αβ complex elutes later as a very large peak with shoulders representing inner arm peaks *d*/*e* to the left and *f*/*g* to the right (Kagami and Kamiya, 1992). In the *sup-pf-2* sample, it is clear that the αβ peak is markedly reduced when compared with wild-type, whereas the γ peak is barely detectable above background. All seven inner arm peaks appear to be present at wild-type levels.

All fractions from both profiles were then analyzed on both 3–5% and 5–15% polyacrylamide gels to identify possible polypeptide defects. Stoichiometrically loaded samples representing the peak fractions from both profiles are shown in Fig. 3, *b* and *c*. Analysis of the DHC region indicates that all inner and outer arm dynein isoforms are present in *sup-pf-2* (Fig. 3 *c*), but the outer arm DHCs are reduced relative to the inner arm subspecies and to the wild-type extracts. Similar results with dynein ICs and LCs were observed on the 5–15% gels (data not shown). These results suggest that *sup-pf-2* axonemes are specifically defective in the outer dynein arms, but that the inner dynein arms are present at approximately wild-type levels.

Structural Defects in sup-pf-2 Axonemes

Since the biochemical data suggested an outer arm deficiency in *sup-pf-2* axonemes, we used thin-section EM to characterize the structural defect. Axonemes were isolated from wild-type and *sup-pf-2* cells and processed for EM as described in Materials and Methods. Preliminary analyses of individual cross-sections revealed that the outer dynein arms were missing from a limited number of doublets in each *sup-pf-2* axoneme (Fig. 4, *c* and *d*), whereas only doublet 1 lacked outer arm structures in wild-type samples processed in parallel (Fig. 4, *a* and *b*).

To obtain a more quantitative estimate of the outer arm defect in *sup-pf-2* axonemes, image averaging procedures

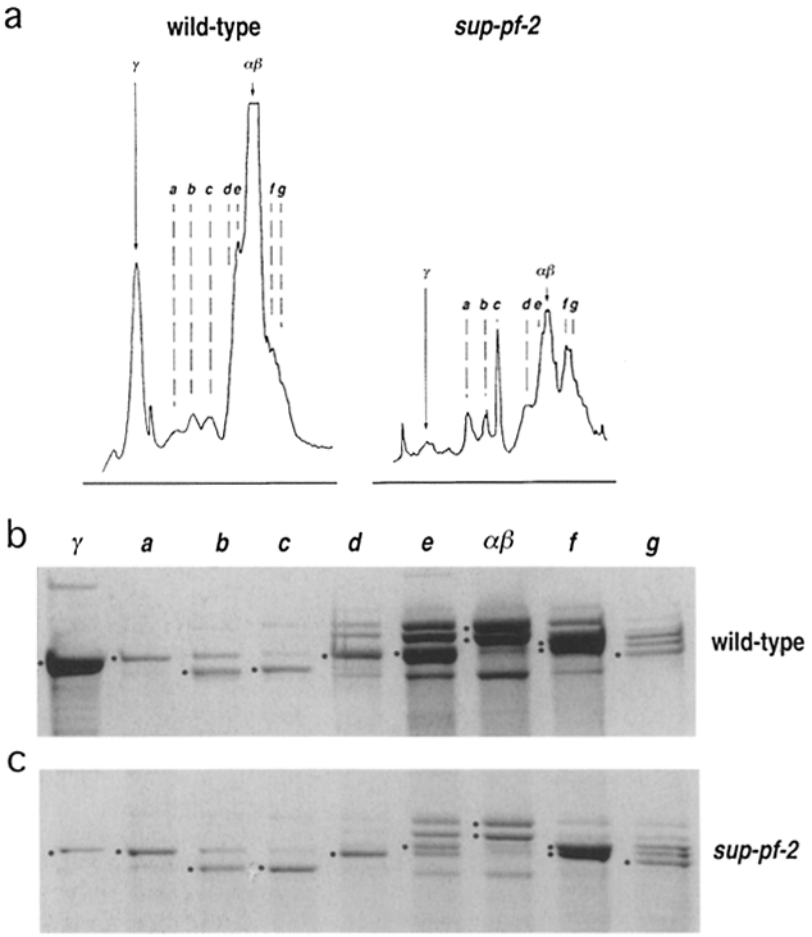

Figure 3. Ion exchange chromatography of dynein extracts. (*a*) Stoichiometric amounts of wild-type and *sup-pf-2* dynein extracts were separated by FPLC on a Mono-Q anion exchange column. The profiles represent the absorbance (280 nm) of the proteins eluted from the column by a 100–400 mM NaCl gradient. Peaks corresponding to the outer arm αβ complex and γ-DHC, and the inner arm isoforms (*a–g*) are indicated on each profile. The αβ- and γ-DHC peaks appear reduced in the *sup-pf-2* profile as compared with wild type. (*b* and *c*) Peak fractions from the wild-type and *sup-pf-2* profiles were analyzed by SDS-PAGE on silver-stained 3–5% acrylamide, 3–8 M urea gradient gels. Only the DHC region of each gel is shown. Each lane was loaded with the same volume to facilitate comparisons between the strains. Since some peaks contain multiple, overlapping heavy chains, the bands corresponding to the principle polypeptides for each dynein isoform are indicated by dots to the left of each lane. The *sup-pf-2* electrophoretic pattern (*c*) clearly shows that all the inner arm DHC isoforms are present; however, the outer arm DHCs are reduced in intensity compared with wild type (*b*). The identity of each peak fraction is indicated at the top in *b*.

(Mastronarde et al., 1992) were used to analyze axoneme cross-sections. Axoneme cross-sections were first preselected based on the presence of an intact central pair apparatus and clearly visible protofilaments on at least one of the axonemal doublets. All outer doublets with clear protofilament substructure were then combined to obtain an average image for a particular strain. Since the mutant strains (*sup-pf-2*, *oda11*, and *pf28*) used in this study have outer dynein arm defects, the images of the outer doublets were normalized to the inner dynein arm densities, a procedure that compensates for small differences in staining intensity between independent preparations of the same sample (for discussion, see Mastronarde et al., 1992). The resultant averages from the *sup-pf-2* cross-sections are shown in Fig. 5 and can be compared with those obtained from wild-type, *oda11*, and *pf28*. The structural defects are most clearly illustrated in the difference plots (Fig. 5, *d*, *f*, and *h*).

As shown in Fig. 5, *c* and *d*, *sup-pf-2* axonemes have an outer arm deficiency that encompasses the entire outer arm region and is not limited to a specific structural domain. This defect is different from that observed with *oda11* (Fig. 5, *e* and *f*), which lacks the α-DHC and its associated LC (see also Sakakibara et al., 1991). The *sup-pf-2* defect is clearly less severe than that observed with *pf28* (Fig. 5, *g* and *h*), a mutant that completely lacks outer arm structures (Mitchell and Rosenbaum, 1985). Averaging of the outer arm deficiencies for individual *sup-pf-2* doublets suggests a 40–45% reduction in outer dynein arms (4.6 ± 1.4 outer arms per cross-section, $n = 151$ axonemes). This estimate correlates well with an ~50% reduction in axonemal ATPase activity measured in isolated *sup-pf-2* axonemes (see Table II). These results are also consistent with functional and biochemical data indicating that the dynein deficiencies in *sup-pf-2* are less dramatic than those observed in mutants completely lacking outer arms, but different from those missing only a portion of the outer arm structure (see Table II).

Since the number of outer doublets lacking outer dynein arms varied slightly among cross-sections, we wanted to determine whether specific doublets were consistently affected or if the defect was random. To acquire this information, individual cross-sections were oriented to allow identification of specific outer doublets using morphological markers (see Materials and Methods). A summary of these results (Fig. 6) indicates that the outer arm deficiency is most pronounced on outer doublets 3 and 6–9, which appear to lack outer arm structures ~50% of the time. The variability in the number of outer arms per cross-section might suggest that the *sup-pf-2* defects occur sporadically along the length of an axoneme, where regions lacking outer arms are interspersed by regions containing outer arms. Despite numerous efforts to address this question, we have been unable to obtain adequate images, using either negative stain EM or immunofluorescence procedures, that clearly depict the longitudinal distribution of

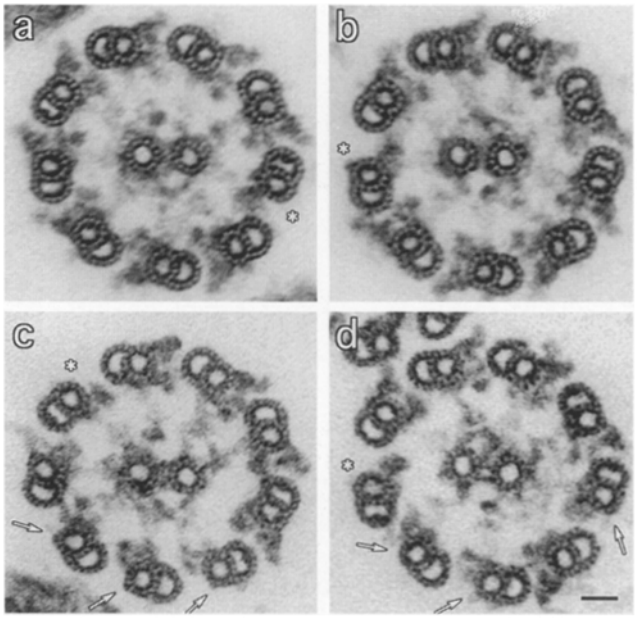

Figure 4. Identification of a structural defect in *sup-pf-2* axonemes. Cross-sections of wild-type (*a* and *b*) and *sup-pf-2* (*c* and *d*) axonemes were analyzed by transmission EM. Each image is from the proximal region of the axoneme as identified by morphological markers. The location of doublet 1 is indicated by asterisks. Additional doublets lacking outer arm structures are indicated by arrows in the *sup-pf-2* images (*c* and *d*). Bar, 25 nm.

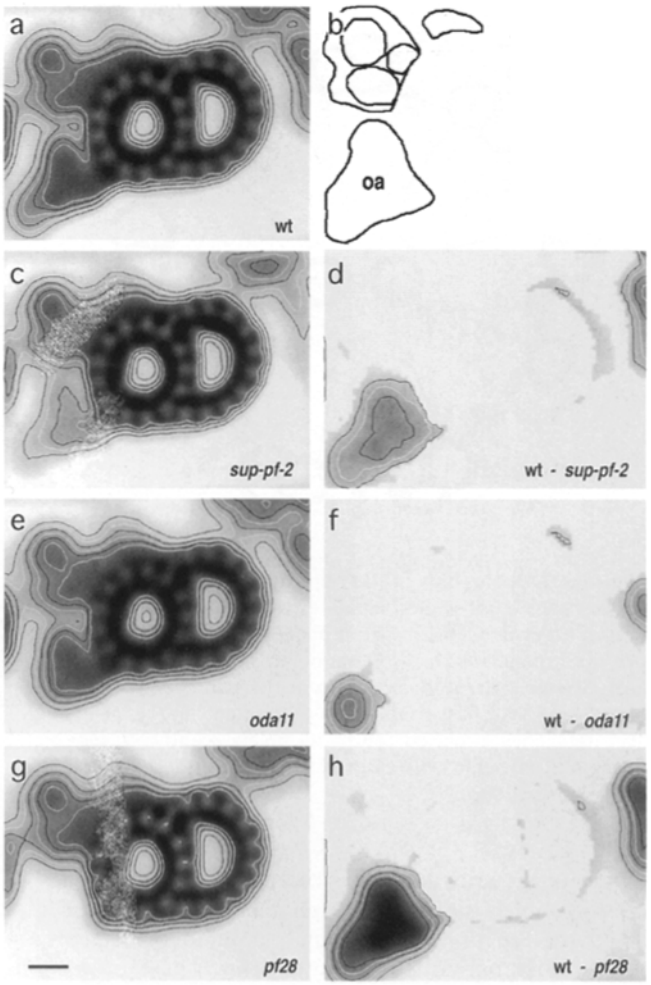

Figure 5. Characterization of the *sup-pf-2* outer arm defect. Grand averages (*a*, *c*, *e*, and *g*) and difference plots (*d*, *f*, and *h*) of random doublet cross-sections from wild-type (*a*), *sup-pf-2* (*c* and *d*), *oda11* (*e* and *f*), and *pf28* (*g* and *h*) axonemes were prepared as described by Mastronarde et al. (1992). The model (*b*) indicates the location of the outer arm (*oa*) densities. The difference plots represent subtractions of the mutant averages from the wild-type average. Differences not significant at the 0.05 confidence level are set to zero. The wt-*pf28* difference plot (*h*) shows a complete loss of outer arm structures, whereas the wt-*oda11* difference plot (*f*) identifies the location of the α-DHC. The wt-*sup-pf-2* difference plot (*d*) indicates that the *sup-pf-2* defect is not limited to a specific outer arm domain. Bar, 10 nm.

outer arms along a single doublet microtubule. In any case, the lack of outer dynein arms on a subset of outer doublets could result from defects in either the doublet microtubules, the outer arm docking structures (Takada and Kamiya, 1994), or the outer dynein arms themselves. To help distinguish between these possibilities, several assays were performed to identify the basis of these defects.

Binding of Wild-type Outer Arms to sup-pf-2 Axonemes

To assess whether the structural defect observed in *sup-pf-2* axonemes could result from a defect in the outer doublet microtubules, unextracted *sup-pf-2* axonemes were assayed for their ability to support the binding of exogenous wild-type outer dynein arms to unoccupied sites on the outer doublets. This assay was performed at various extract/axoneme stoichiometries (see Materials and Methods). Both the 1:1 and 2:1 ratios represented a substantial excess of exogenously added dynein relative to the number of unoccupied binding sites available on unextracted *sup-pf-2* or wild-type axonemes. The addition of wild-type dynein extracts at a 1:1 stoichiometry increased the amount of dynein bound in both wild-type and *sup-pf-2* samples. Structurally, this correlates with an increase in the number of outer doublets bearing outer dynein arms (Fig. 7). *sup-pf-2* axonemes increased from an average of five to six doublets bearing outer arms in control samples to eight to nine doublets in dynein-treated samples. The increase observed with wild-type axonemes resulted from the addition of outer arms to doublet 1, which is normally unoccupied in vivo (Hoops and Witman, 1983). Binding of dynein arms to other sites on the outer doublets was not observed, most likely because binding by the ATP-sensitive site was prevented by addition of vanadate to the dynein extracts (see Materials and Methods). These experiments suggest that a defect in the *sup-pf-2* outer doublets is unlikely because the wild-type outer arms could bind to the vacant sites in the *sup-pf-2* axonemes. However, because the wild-type dynein extracts also contained wild-type docking proteins (Takada and Kamiya, 1994), a defect in the *sup-pf-2* docking structures might not have been revealed in these experiments.

Presence of an Outer Arm Docking Projection

To determine if *sup-pf-2* axonemes have a potential defect

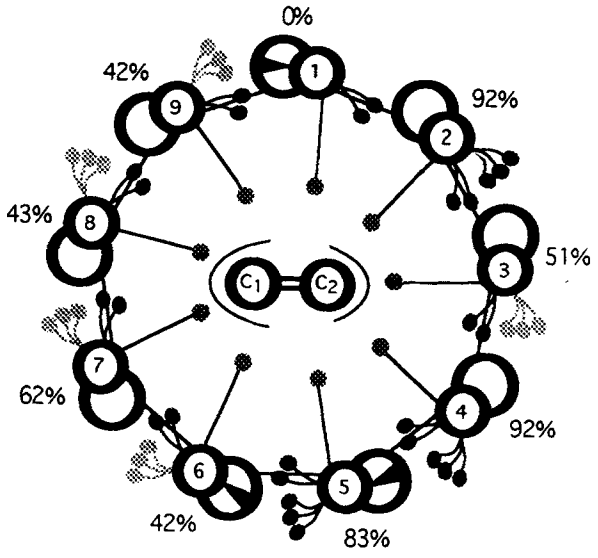

Figure 6. Doublet bias of the outer arm defect. This diagram of an axoneme cross-section indicates the doublet-specific distribution of outer dynein arms from images of the proximal region of *sup-pf-2* axonemes (n = 53 axonemes). The numbers listed by each doublet microtubule represent the percentage of time that outer arms were observed on those doublets. Note that the outer arm deficiency is biased toward doublets 3 and 6–9. Doublet 1 rarely has an outer arm, even in wild-type preparations (Hoops and Witman, 1983).

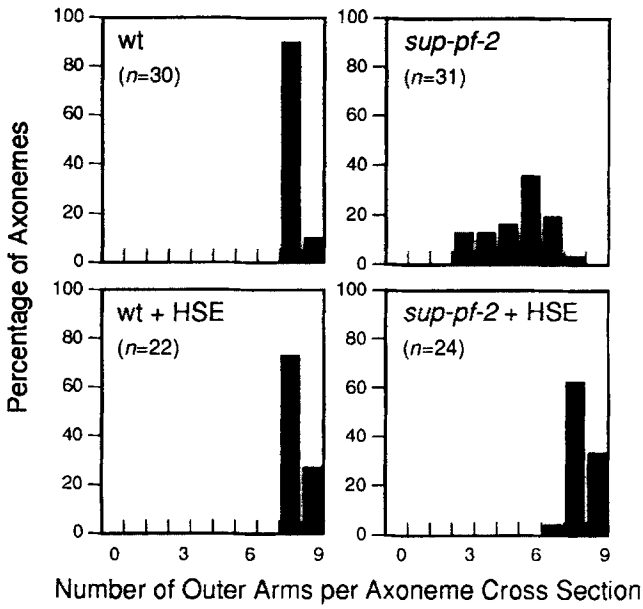

Figure 7. Binding of exogenous outer arms to unoccupied sites on wild-type and *sup-pf-2* axonemes. Wild-type dynein extracts (*HSE*), containing 0.5 mM ATP and 100 μM vanadate, were incubated with unextracted wild-type (*wt*) and *sup-pf-2* axonemes at extract/axoneme stoichiometries of 0:1 (control) and 1:1. Samples were fixed and analyzed by EM to determine the location of dynein addition. Images of axonemes were analyzed for the number of outer arms bound per cross-section. When dynein was added to wild-type axonemes (*wt + HSE*), there was a slight increase in the number of axonemes possessing nine outer arms per cross-section. When dynein was added to *sup-pf-2* axonemes, there was a dramatic increase in the number of outer arms bound per cross-section (*sup-pf-2 + HSE*) compared with controls (*sup-pf-2*). Binding to abnormal locations on the outer doublets was not observed. The number of axonemal cross-sections examined (n) is indicated for each sample.

in the outer arm docking structures, random images of cross-sections from *sup-pf-2* and *pf28* axonemes were analyzed for the presence of small pointed projections on those doublets that lacked outer arms. These projections have been correlated with the presence of components required for binding outer arms to the outer doublets (Takada and Kamiya, 1994) and are apparent in cross-sections from both *pf28* (Fig. 8 *a*) and *sup-pf-2* axonemes (Fig. 8 *b*). Image averages obtained from outer doublets in *pf28* and *sup-pf-2* axonemes that lacked outer dynein arms show virtually identical projections (Fig. 8, *c* and *d*).

To investigate the frequency with which the projections appear on individual outer doublets, images of cross-sections from *sup-pf-2* and *pf28* axonemes were scored for the presence or absence of the projection (Table III). This analysis was limited to the proximal region where doublet number could be positively identified by the presence of specific morphological markers. Projections were observed on doublets 2–9 in both the *sup-pf-2* and *pf28* samples 45–60% of the time. Interestingly, doublet 1 rarely displayed a projection, which may account for the lack of outer arm structures on this doublet in all strains (data not shown). Why then do *sup-pf-2* axonemes lack outer arms on some doublets? Is the activity of the docking proteins altered in *sup-pf-2* cells? To address this question, we decided to look at the relationship between the *sup-pf-2* mutation and other mutations that have been associated with defects in the docking structures.

Relationship between sup-pf-2 and Other oda Mutations

Axonemes from *oda1* and *oda3* cells lack outer dynein arms as well as the putative outer arm docking structures and their associated polypeptides, and they cannot bind purified outer dynein arms unless a 7S factor that contains two polypeptides of 105 and 70 kD is also included (Kamiya, 1988; Takada and Kamiya, 1994). Thus, a defect in the docking projection polypeptides appears to be responsible for the loss of outer dynein arms in these mutants. To determine whether the *sup-pf-2* mutation might be related to either *oda1* or *oda3*, we decided to perform complementation tests with these strains.

To construct stable diploid cell lines for complementation tests, each motility mutation was first crossed into either an *arg2* or *arg7* background. The initial cross of *sup-pf-2* with *arg2* indicated that the previous assignment of the *SUP-PF-2* locus to linkage group I (Huang et al., 1982) was incorrect. Given this result, we decided to expand our complementation analysis to include most of the known *oda* mutations. The gene products of several of the *ODA* loci have been identified (see Table I). The *sup-pf-2 arg2* strain was mated to the appropriate *oda arg7* strains, and stable diploid cell lines were selected on medium lacking arginine. The resulting diploid cells were then examined by phase-contrast microscopy, and their swimming velocities were compared to the swimming velocities of their haploid parents. Wild-type swimming velocity was observed in all

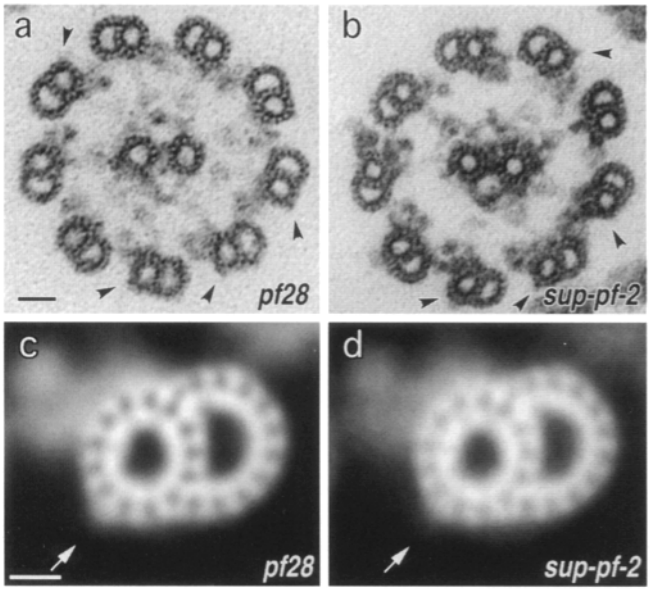

Figure 8. Presence of an outer doublet projection. Micrographs of *pf28* (*a*) and *sup-pf-2* (*b*) axoneme cross-sections were analyzed for the presence of a small, pointed structure at the site where outer arms are normally bound. Several outer doublets in each strain clearly show this small projection (*arrowheads*). Averages of *pf28* (*c*) and *sup-pf-2* (*d*) doublets that lack outer arms were prepared to better compare the putative outer arm docking structure (*arrows*) between these strains. The images are presented in negative contrast for better visualization of the doublet projections. No obvious differences in the projection domains were detected between *pf28* and *sup-pf-2*. Bars: (*a* and *b*) 25 nm; (*c* and *d*) 10 nm.

of the *sup-pf-2/oda* diploids with the exception of the *sup-pf-2/pf28* diploids, which displayed a swimming velocity similar to the *sup-pf-2* parent strain (75.2 ± 12 μm/s, n = 50 cells; Table IV). This failure to complement suggests that the *sup-pf-2* and *pf28 (oda2)* mutations may be alleles at the same locus. To confirm this observation, we tested the *sup-pf-2* mutation for linkage to markers on linkage group XI. The *sup-pf-2* parent strain was first mated to *ery1*, a drug resistance marker located on the right arm of linkage group XI. Recombination analysis of the resulting tetrad progeny indicated that the *sup-pf-2* mutation maps to linkage group XI, ~20 centimorgans (cM) from *ery1* (Table IV). We then mated *sup-pf-2* to *pf28* directly; no recombinants were observed in 25 complete tetrads (Table IV). Both the absence of recombination and the failure to complement indicate that *pf28* and *sup-pf-2* are alleles at the same locus.

Table III. Occurrence of Outer Doublet Projections

Strain	Doublets with (+) or without (−) a projection			
	+	−	±*	Doublets counted‡
	%			
sup-pf-2	60.2	23.8	16	176
pf28	44	14.1	41.9	248

*Doublets in which the presence or absence of a projection was ambiguous.
‡Projections were scored only on doublets 2–9 from the proximal region.

Table IV. Recombination, Dominance, and Complementation Analysis

Recombination tests	Segregation (PD:NPD:TT)	Conclusions
sup-pf-2-1 X *arg2*	10:3:5	Unlinked
sup-pf-2-1 X *ery1*	13:0:9	~20.5 cM apart
sup-pf-2-1 X *pf28*	25:0:0	<1.9 cM apart
sup-pf-2-1 pf1 X *sup-pf-2-2 pf1*	34:0:0	<1.4 cM apart
sup-pf-2-1 pf1 X *sup-pf-2-3 pf1*	33:0:0	<1.5 cM apart

Dominance tests

Diploid genotype	Motility phenotype*	Conclusions
sup-pf-2-1 arg2 / *SUP-PF-2 arg7*	wild type	*sup-pf-2-1* is recessive
sup-pf-2-2 arg2 / *SUP-PF-2 arg7*	wild type	*sup-pf-2-2* is recessive
sup-pf-2-3 arg7 / *SUP-PF-2 arg2*	wild type	*sup-pf-2-3* is recessive

Complementation tests

Diploid genotype	Motility phenotype*	Conclusions
sup-pf-2-1 arg2 / *sup-pf-2-3 arg7*	like *sup-pf-2-3*	Alleles at same locus
sup-pf-2-1 arg2 / *pf28 arg7*	like *sup-pf-2-1*	Alleles at same locus
sup-pf-2-2 arg2 / *pf28 arg7*	like *sup-pf-2-2*	Alleles at same locus
sup-pf-2-3 arg7 / *pf28 arg2*	like *sup-pf-2-3*	Alleles at same locus

*Diploid motility phenotypes were scored by visual assessment of swimming velocity, compared with both its haploid parents and wild-type, and/or measurement of flagellar beat frequency.

Characterization of New sup-pf-2 Alleles

Screens for mutations that restore motility to the paralyzed, radial spoke defective strain, *pf1*, have recently resulted in the recovery of several new extragenic suppressors (Mitchell, B., manuscript in preparation). 11 of these suppressors appear to be new alleles of the *SUP-PF-2* locus (see Materials and Methods). After recovery of these strains in a wild-type background, it became apparent that their motility phenotypes fell into two distinct groups with different beat frequency ranges, one at 28–30 Hz and another at 48–50 Hz. We chose to analyze two strains (S3 and S14), one from each beat frequency group, based on the assumption that allele-specific differences might be more evident between strains with widely differing beat frequencies.

To confirm that the different motility phenotypes observed were representative of alleles at the *SUP-PF-2/PF28* locus, the two new mutations were tested for allelism with *pf28* and the original *sup-pf-2* mutation (now designated *sup-pf-2-1*) by recombination and complementation tests. Both the *sup-pf-2-2* (S14) and *sup-pf-2-3* (S3) alleles failed to recombine with the *sup-pf-2-1* mutation in >33 tetrads (Table IV). In addition, complementation analysis

Table V. Motility and Structural Phenotypes of sup-pf-2 Mutations

Strain (isolate)	Beat frequency	Swimming velocity	Number of outer arms per cross-section
	Hz	*μm/s*	
sup-pf-2-1	40	70.7 ± 9.8 (n = 100)	4.6 ± 1.4 (n = 151)
sup-pf-2-2 (S14)	49	90 ± 12.5 (n = 100)	6.1 ± 1.4 (n = 68)
sup-pf-2-3 (S3)	28	110 ± 20.3 (n = 100)	7.8 ± 0.5 (n = 32)

Swimming velocity and the number of outer arms per cross-section are expressed as mean ± SD.

indicates that the motility phenotypes of all of the *sup-pf-2* mutations are recessive with respect to the wild-type *SUP-PF-2* allele, but all are dominant with respect to the *pf28* mutation. These results demonstrate that the different mutant alleles at the *SUP-PF-2/PF28* locus can display a broad range of motility phenotypes.

To determine how the different motility phenotypes might be related to the state of outer arm assembly, *sup-pf-2-2* and *sup-pf-2-3* axonemes were examined by thin-section EM. The results of this analysis are summarized in Table V. Both *sup-pf-2-2* and *sup-pf-2-3* differ from *sup-pf-2-1* with respect to beat frequency and swimming velocity. However, the most striking difference between the three strains is the number of outer arms that are observed in axoneme cross-sections. *sup-pf-2-2* axonemes have more outer arms present per cross-section than *sup-pf-2-1* axonemes, consistent with both its faster beat frequency and swimming velocity. Interestingly, the bias of outer arm loss on specific outer doublets is preserved between the strains (data not shown; see Fig. 6). In contrast, axonemes from *sup-pf-2-3* cells, which have a reduced beat frequency, show no significant outer arm assembly defects. These results indicate that the outer arm assembly defects in *sup-pf-2* strains vary in an allele-specific manner.

Discussion

The sup-pf-2 Mutations Alter the Activity of the Dynein Arms

In the early 1980's, a group of bypass suppressor mutations were identified that were capable of restoring partial motility to paralyzed radial spoke or central pair defective strains without restoring the original missing structures (Huang et al., 1982). More recent work has shown that most of these suppressor mutations alter components of the inner dynein arms or the dynein regulatory complex (Piperno et al., 1992, 1994; Porter et al., 1992; Gardner et al., 1994). In this study, we report several lines of evidence that indicate that the *sup-pf-2* mutations, similar to the *sup-pf-1* mutations (Brokaw et al., 1982; Porter et al., 1994), alter outer dynein arm activity. First, the *sup-pf-2* mutations result in a reduction in swimming velocity and flagellar beat frequency (see Tables II and V). Reductions in these functional parameters are suggestive of outer arm defects. Second, biochemical analyses of *sup-pf-2-1* axonemes show that the outer arm polypeptides are reduced to 55–60% of wild-type levels (Figs. 1-3 and 7). In contrast, the inner arm DHCs appear to be present at nearly wild-type levels (Fig. 3). Additionally, *sup-pf-2-1* axonemal ATPase activity is reduced to ~50% of wild-type levels (Table II), consistent with a defect in outer dynein arm activity. Third, structural analysis of axoneme cross-sections reveals that the number of outer dynein arms observed on the outer doublet microtubules is reduced in some *sup-pf-2* alleles as compared with wild type (Figs. 4 and 6; Table V). This defect reflects a uniform loss of outer arm structure that is not concentrated to a particular domain (Figs. 4 and 5). Interestingly, the outer arm structural defect appears to be biased toward a subset of outer doublets. By examining cross-sectional images obtained from the proximal region of *sup-pf-2-1* axonemes, we have been able to identify doublets 3, 6, 8, and 9 as being the most severely affected, possessing outer arms ≤50% of the time (see Fig. 6). This defect results in a radial asymmetry in the distribution of outer dynein arms. Based on evidence from dynein rebinding assays and detailed image analysis of axoneme cross-sections, the structural defect does not result from defects in either the outer doublet microtubules or the putative outer arm docking structures, but rather appears to result from a defect in the outer dynein arms themselves (Figs. 7 and 8).

The sup-pf-2 Mutations Alter the γ-DHC

To test whether the *sup-pf-2* mutations are related to any of the known outer dynein arm mutations, complementation tests were performed in stable diploid cell lines. Each *sup-pf-2* mutation tested failed to complement the *pf28* mutation (Table IV). In addition, recombination analysis has shown that the *sup-pf-2-1* and *pf28* mutations are tightly linked to one another. These results indicate that *sup-pf-2* and *pf28* represent two different classes of mutant alleles at the same locus. Based on restriction fragment length polymorphism mapping data, Wilkerson et al. (1994) have proposed that the *PF28/ODA2* locus encodes the structural gene for the outer arm γ-DHC. Recent Southern blot analysis of numerous new alleles of *pf28* generated by insertional mutagenesis supports this hypothesis (Mitchell, D., personal communication). Restriction fragment length polymorphisms were observed in several *pf28* alleles when wild-type and mutant DNA samples were hybridized with γ-DHC probes. Taken together, these data indicate that the *sup-pf-2* mutations represent defects in the gene that encodes the outer arm γ-DHC.

Interestingly, mapping the *sup-pf-2* mutation to the structural gene for the outer arm γ-DHC is consistent with two additional observations. First, a relatively large number of *sup-pf-2* alleles has been recovered after UV-induced mutagenesis of *pf1* cells (Mitchell, B., manuscript in preparation). This suggests that the *SUP-PF-2* locus is a large target, similar to what might be expected from a large DHC gene. Second, analysis of dynein extracts fractionated by sucrose density centrifugation indicates that the 12S peak of ATPase activity is reduced in *sup-pf-2-1*. These results would be consistent with an alteration in γ-DHC activity. The *sup-pf-2* mutations therefore represent a special class of γ-DHC mutations that appear to assemble a modified outer dynein arm.

Comparison with Other DHC Mutants

Mutations in any of the thirteen different loci can disrupt the assembly of the outer dynein arms (Huang et al., 1979; Kamiya, 1988; Sakakibara et al., 1991). Most *oda* mutations result in complete loss of outer arms and appear to be produced by defects in specific outer arm components (see Table I). However, defects in DHC components appear to have a broad range of effects on the assembly of the outer arm. The α-DHC locus is represented by the single *oda11* allele; this mutation results in loss of only a single heavy chain (α-DHC) and its associated 16-kD LC but does not alter the assembly of the remaining outer arm components (Sakakibara et al., 1991). The β-DHC locus is represented by several *oda4* alleles, most of which fail to assemble the outer arm. Interestingly, the *oda4-s7* mutation, which produces a truncated β-DHC, supports only partial assembly of outer arms that lack one of the three globular heads (Sakakibara et al., 1993). In contrast, the *sup-pf-1* mutations, which alter the activity of the β-DHC, support assembly of a wild-type complement of outer arms (Huang et al., 1982; Porter et al., 1994). The γ-DHC locus is represented by multiple *pf28/oda2* alleles that fail to assemble the outer arms (Kamiya, 1988; Mitchell and Rosenbaum, 1985) and, as shown here, by the *sup-pf-2* alleles that display partial outer arm assembly. Thus, while some outer arm DHC mutations will support some level of outer arm assembly, the extent of outer arm assembly varies between these strains. In particular, the extent of outer arm assembly observed in *sup-pf-2* strains appears to vary in an allele-specific manner (see Table V). These results suggest that the γ-DHC, in addition to the β-DHC, appears to play an important role in stabilizing the outer dynein arms.

Why some *sup-pf-2* axonemes display a radially asymmetric distribution of outer dynein arms remains unresolved. We can only speculate that the asymmetry may reflect some aspect of outer arm and/or γ-DHC assembly. Interestingly, radial asymmetries within the axoneme have previously been revealed by analysis of other *Chlamydomonas* mutant strains. The inner arm mutant *bop2-1*, which was isolated as a specific suppressor of paralyzed *pf10* cells, is missing an inner arm structure that appears to be restricted to specific doublets (King et al., 1994). In addition, the *mbo* class of mutants, which can only swim backwards, lacks B-tubule projections in doublets 1, 5, and 6 (Segal et al., 1984). The causes of these asymmetries also remain unresolved.

Possible Mechanisms of Suppression

To generate an efficient flagellar waveform, the activity of the multiple dynein motors must be somehow coupled and selectively activated and inhibited at different points in the beat cycle. Such a process may involve cooperative interactions between dynein arms, a mechanochemical feedback mechanism (see Brokaw, 1971; Lindemann, 1994*a*,*b*), and/or the transmission of signals from key axoneme components. Several lines of structural and genetic evidence implicate the central pair (CP) and radial spoke (RS) structures as modulators of dynein arm activity (for reviews see Smith and Sale, 1994; Porter, 1996). CP and RS deficient strains (*pf* strains) are paralyzed under physiological conditions (Witman et al., 1978) and display reduced microtubule sliding velocities in sliding disintegration assays (Smith and Sale, 1992*a*). The decrease in sliding velocity appears to be mediated in part by phosphorylation of the inner dynein arms (Smith and Sale, 1992*b*; Howard et al., 1994; Habermacher and Sale, 1995, 1996). However, inhibition of phosphorylation is not sufficient to restore flagellar motility in *pf* strains (Howard et al., 1994). This result suggests that other components within the axoneme must also be inhibiting dynein arm activity in CP/RS mutants. Interestingly, suppressed *pf* strains (e.g., *sup-pf-1 pf14*, *sup-pf-2-1 pf14*, *sup-pf-3 pf14*, and *sup-pf-4 pf14*) display near wild-type sliding velocities (Smith and Sale, 1992*a*; Rupp, G., G. Habermacher, W. Sale, and M.E. Porter, unpublished observations), and the sliding velocity of *sup-pf-2-1 pf14* is unaffected by either kinase or phosphatase inhibitors (Rupp, G., G. Habermacher, W. Sale, and M.E. Porter, unpublished observations). These results may indicate that motility is restored in the suppressed strains by a mechanism that overrides inhibitory phosphorylation signals.

Other recent studies have suggested that the CP/RS structures are important for overriding inhibitory signals from proposed regulatory nucleotide binding sites (Kinoshita et al., 1995; Omoto et al., 1996). The working hypothesis is that high concentrations of ATP (1 mM) inhibit dynein-induced sliding by binding to such a regulatory site. In wild-type flagella, signals from the CP/RS complex relieve this inhibition in a coordinated manner, but, in *pf* mutants, physiological levels of ATP inhibit movement. The location of the proposed regulatory nucleotide binding site(s) has not been determined, but it has been postulated that such site(s) might reside in either the β-DHC and/or γ-DHC (Omoto et al., 1996), perhaps in one or more of the four P-loop domains that have been identified by DHC sequence analysis (for review see Gibbons, 1995). Although it is still unknown where the *sup-pf-2* mutations fall within the γ-DHC gene, one intriguing possibility is that the *sup-pf-2* mutations may affect one of the four γ-DHC P-loops. In support of this hypothesis, the extensive sliding disintegration pattern that can be induced in wild-type axonemes only by reducing [ATP] below 50 mM (Omoto et al., 1996) has been observed with *sup-pf-2-1 pf14* axonemes in the presence of high [ATP] (~1 mM; Rupp, G., G. Habermacher, W. Sale, and M.E. Porter, unpublished observations). Significantly, this pattern has not been observed with other suppressed *pf14* strains under the same conditions. It is therefore possible that the *sup-pf-2* mutations may affect a regulatory nucleotide binding site directly and/or another domain of the γ-DHC that responds to signals from this site. Further analysis of the *sup-pf-2* alleles will be needed to address these questions and to better define the domains of the DHCs that regulate dynein arm activity.

This manuscript is dedicated to Dr. Samuel M. McGee-Russell on the occasion of his retirement from the State University of New York at Albany. His enthusiastic approach to teaching, love of scientific investigation, and continuous encouragement served as the inspiration for one of us (G. Rupp) to pursue a career in cell biology.

The authors wish to acknowledge Dave Mitchell for sharing insightful ideas, unpublished observations, and several double mutant strains. We also thank Charlotte Omoto and Pete Lefebvre for helpful discussions, Tom Giddings for assistance with EM, Win Sale and Geoff Habermacher

for instruction and assistance with sliding disintegration assays, and members of the Porter laboratory for constructive comments on this manuscript.

This work was supported by grants from the National Science Foundation (NSF) (MCB9305217) and the March of Dimes (FY95-1031) to M.E. Porter, and by a National Institutes of Health (NIH) fellowship (F32-GM17902) to G. Rupp. Additional support was from an NSF research training grant in Cytoskeletal Biology (91-11-44, R. Linck, P.I.) and the Minnesota Medical Foundation grant MRF-115-96. Eileen O'Toole was supported by NIH grant RR00592 to the Boulder Laboratory for Three-dimensional Fine Structure (J.R. McIntosh, director).

Received for publication 27 June 1996 and in revised form 25 October 1996.

References

Bradford, M. 1976. A rapid and sensitive method for quantitation of microgram quantities of proteins utilizing the principle of protein-dye binding. *Anal. Biochem.* 72:248–254.

Brokaw, C.J. 1971. Bend propagation by a sliding filament model for flagella. *J. Exp. Biol.* 55:289–304.

Brokaw, C.J., and R. Kamiya. 1987. Bending patterns of *Chlamydomonas* flagella: IV. Mutants with defects in inner and outer dynein arms indicate differences in dynein arm function. *Cell Motil. Cytoskeleton.* 8:68–75.

Brokaw, C.J., and D.J.L. Luck. 1985. Bending patterns of *Chlamydomonas* flagella. III. A radial spoke head deficient mutant and a central pair deficient mutant. *Cell Motil.* 5:195–208.

Brokaw, C.J., D.J.L. Luck, and B. Huang. 1982. Analysis of the movement of *Chlamydomonas* flagella: the function of the radial-spoke system is revealed by comparison of wild-type and mutant flagella. *J. Cell Biol.* 92:722–732.

Ebersold, W.T. 1967. *Chlamydomonas reinhardtii*: Heterozygous diploid strains. *Science (Wash. DC).* 157:446–449.

Fox, L.A., and W.S. Sale. 1987. Direction of force generated by the inner row of dynein arms on flagellar microtubules. *J. Cell Biol.* 105:1781–1787.

Gardner, L.C., E. O'Toole, C.A. Perrone, T. Giddings, and M.E. Porter. 1994. Components of a "dynein regulatory complex" are located at the junction between the radial spokes and the dynein arms in *Chlamydomonas* flagella. *J. Cell Biol.* 127:1311–1325.

Gibbons, I.R. 1995. Dynein family of motor proteins: present status and future questions. *Cell Motil. Cytoskeleton.* 32:136–144.

Goodenough, U.W., B. Gebhart, V. Mermall, D.R. Mitchell, and J.E. Heuser. 1987. High-pressure liquid chromatography fractionation of *Chlamydomonas* dynein extracts and characterization of inner-arm dynein subunits. *J. Mol. Biol.* 194:481–494.

Habermacher, G., and W.S. Sale. 1995. Regulation of dynein-driven microtubule sliding by an axonemal kinase and phosphatase in *Chlamydomonas* flagella. *Cell Motil. Cytoskeleton.* 32:106–109.

Habermacher, G., and W.S. Sale. 1996. Regulation of flagellar dynein by an axonemal type-1 phosphatase in *Chlamydomonas*. *J. Cell Sci.* 109:1899–1907.

Holmes, J.A., and S.K. Dutcher. 1989. Cellular asymmetry in *Chlamydomonas reinhardtii*. *J. Cell Sci.* 94:273–285.

Hoops, H.J., and G.B. Witman. 1983. Outer doublet heterogeneity reveals structural polarity related to beat direction in *Chlamydomonas* flagella. *J. Cell Biol.* 97:902–908.

Howard, D.R., G. Habermacher, D.B. Glass, E.F. Smith, and W.S. Sale. 1994. Regulation of *Chlamydomonas* flagellar dynein by an axonemal protein kinase. *J. Cell Biol.* 127:1683–1692.

Huang, B., G. Piperno, and D.J.L. Luck. 1979. Paralyzed flagellar mutants of *Chlamydomonas reinhardtii* defective for axonemal doublet microtubule arms. *J. Biol. Chem.* 254:3091–3099.

Huang, B., Z. Ramanis, and D.J.L. Luck. 1982. Suppressor mutations in *Chlamydomonas* reveal a regulatory mechanism for flagellar function. *Cell.* 28: 115–125.

Kagami, O., and R. Kamiya. 1990. Strikingly low ATPase activities in flagellar axonemes of a *Chlamydomonas* mutant missing outer dynein arms. *Eur. J. Biochem.* 187:441–446.

Kagami, O., and R. Kamiya. 1992. Translocation and rotation of microtubules caused by multiple species of *Chlamydomonas* inner-arm dynein. *J. Cell Sci.* 103:653–664.

Kamiya, R. 1982. Extrusion and rotation of the central-pair microtubules in detergent-treated *Chlamydomonas* flagella. *Cell Motil.* 1 (Suppl.):169–173.

Kamiya, R. 1988. Mutations at twelve independent loci result in absence of outer dynein arms in *Chlamydomonas reinhardtii*. *J. Cell Biol.* 107:2253–2258.

Kamiya, R., E. Kurimoto, and E. Muto. 1991. Two types of *Chlamydomonas* flagellar mutants missing different components of inner-arm dynein. *J. Cell Biol.* 112:441–447.

King, S.J., W.B. Inwood, E.T. O'Toole, J. Power, and S.K. Dutcher. 1994. The *bop2-1* mutation reveals radial asymmetry in the inner dynein arm region of *Chlamydomonas reinhardtii*. *J. Cell Biol.* 126:1255–1266.

Kinoshita, S., T. Miki-Noumura, and C.K. Omoto. 1995. Regulatory role of nucleotides in axonemal function. *Cell Motil. Cytoskeleton.* 32:46–54.

Laemmli, U. K. 1970. Cleavage of structural proteins during the assembly of the head of bacteriophage T4. *Nature (Lond.).* 227:680–685.

Levine, R.P., and W.T. Ebersold. 1960. The genetics and cytology of *Chlamydomonas*. *Annu. Rev. Microbiol.* 14:197–216.

Lindemann, C.B. 1994*a*. A "geometric clutch" hypothesis to explain oscillations of the axoneme of cilia and flagella. *J. Theor. Biol.* 168:175–189.

Lindemann, C. B. 1994*b*. A model of flagellar and ciliary functioning which uses the forces transverse to the axoneme as the regulator of dynein activation. *Cell Motil. Cytoskeleton.* 29:141–154.

Luck, D.J.L., G. Piperno, Z. Ramanis, and B. Huang. 1977. Flagellar mutants of *Chlamydomonas*: studies of radial spoke-defective strains by dikaryon and revertant analysis. *Proc. Natl. Acad. Sci. USA.* 74:3456–3460.

Mastronarde, D.N., E.T. O'Toole, K.L. McDonald, J.R. McIntosh, and M.E. Porter. 1992. Arrangement of inner dynein arms in wild-type and mutant flagella of *Chlamydomonas*. *J. Cell Biol.* 118:1145–1162.

Minoura, I., and R. Kamiya. 1995. Strikingly different propulsive forces generated by different dynein-deficient mutants in viscous media. *Cell Motil. Cytoskeleton.* 31:130–139.

Mitchell, D.R. 1994. Cell and molecular biology of flagellar dyneins. *Int. Rev. Cytol.* 155:141–180.

Mitchell, D.R., and Y. Kang. 1991. Identification of *oda6* as a *Chlamydomonas* dynein mutant by rescue with the wild-type gene. *J. Cell Biol.* 113:835–842.

Mitchell, D.R., and J.L. Rosenbaum. 1985. A motile *Chlamydomonas* flagellar mutant that lacks outer dynein arms. *J. Cell Biol.* 100:1228–1234.

Omoto, C.K., and C. Kung. 1979. The pair of central tubules rotates during ciliary beat in *Paramecium*. *Nature (Lond.).* 279:532–534.

Omoto, C.K., and G.B. Witman. 1981. Functionally significant central pair rotation in a primitive eukaryotic flagellum. *Nature (Lond.).* 290:708–710.

Omoto, C.K., T. Yagi, E. Kurimoto, and R. Kamiya. 1996. Ability of paralyzed flagella mutants of *Chlamydomonas* to move. *Cell Motil. Cytoskeleton.* 33: 88–94.

Pfister, K.K., and G.B. Witman. 1984. Subfractionation of *Chlamydomonas* 18S dynein into two unique subunits containing ATPase activity. *J. Biol. Chem.* 259:12072–12080.

Piperno, G., and D.J.L. Luck. 1979. Axonemal adenosine triphosphatases from flagella of *Chlamydomonas reinhardtii*. Purification of two dyneins. *J. Biol. Chem.* 254:3084–3090.

Piperno, G., and Z. Ramanis. 1991. The proximal portion of *Chlamydomonas* flagella contains a distinct set of inner dynein arms. *J. Cell Biol.* 112:701–709.

Piperno, G., Z. Ramanis, E.F. Smith, and W.S. Sale. 1990. Three distinct inner dynein arms in *Chlamydomonas* flagella: molecular composition and location in the axoneme. *J. Cell Biol.* 110:379–389.

Piperno, G., K. Mead, and W. Shestak. 1992. The inner dynein arms I2 interact with a "dynein regulatory complex" in *Chlamydomonas* flagella. *J. Cell Biol.* 118:1455–1463.

Piperno, G., K. Mead, M. LeDizet, and A. Moscatelli. 1994. Mutations in the "dynein regulatory complex" alter the ATP-insensitive binding sites for inner arm dyneins in *Chlamydomonas* axonemes. *J. Cell Biol.* 125:1109–1117.

Porter, M.E. 1996. Axonemal dyneins: assembly, organization, and regulation. *Curr. Opin. Cell Biol.* 8:10–17.

Porter, M.E., J. Power, and S.K. Dutcher. 1992. Extragenic suppressors of paralyzed flagellar mutations in *Chlamydomonas reinhardtii* identify loci that alter the inner dynein arms. *J. Cell Biol.* 118:1163–1176.

Porter, M.E., J.A. Knott, L.C. Gardner, D.K. Mitchell, and S.K. Dutcher. 1994. Mutations in the *SUP-PF-1* locus of *Chlamydomonas reinhardtii* identify a regulatory domain in the β-dynein heavy chain. *J. Cell Biol.* 126:1495–1507.

Sager, R., and S. Granick. 1953. Nutritional studies in *Chlamydomonas reinhardtii*. *Ann. NY Acad. Sci.* 56:831–838.

Sakakibara, H., D.R. Mitchell, and R. Kamiya. 1991. A *Chlamydomonas* outer arm dynein mutant missing the α heavy chain. *J. Cell Biol.* 113:615–622.

Sakakibara, H., S. Takada, S.M. King, G.B. Witman, and R. Kamiya. 1993. A *Chlamydomonas* outer arm dynein mutant with a truncated β heavy chain. *J. Cell Biol.* 122:653–661.

Sale, W.S., and P. Satir. 1977. The direction of active sliding of microtubules in *Tetrahymena* cilia. *Proc. Natl. Acad. Sci. USA.* 74:2045–2049.

Segal, R.A., B. Huang, Z. Ramanis, and D.J.L. Luck. 1984. Mutant strains of *Chlamydomonas reinhardtii* that move backwards only. *J. Cell Biol.* 98:2026–2034.

Smith, E.F., and W.S. Sale. 1992*a*. Regulation of dynein-driven microtubule sliding by the radial spokes in flagella. *Science (Wash. DC).* 257:1557–1559.

Smith, E.F., and W.S. Sale. 1992*b*. Structural and functional reconstitution of inner dynein arms in *Chlamydomonas* flagellar axonemes. *J. Cell Biol.* 117: 573–581.

Smith, E.F., and W.S. Sale. 1994. Mechanisms of flagellar movement: functional interactions between dynein arms and the radial spoke–central apparatus complex. *In* Microtubules. J.A. Hyams and C.W. Lloyd, editors. Wiley-Liss, New York. 381–392.

Takada, S., and R. Kamiya. 1994. Functional reconstitution of *Chlamydomonas* outer dynein arms from α-β and γ subunits: requirement of a third factor. *J. Cell Biol.* 126:737–745.

Warner, F.D., and P. Satir. 1974. The structural basis of ciliary bend formation. Radial spoke positional changes accompanying microtubule sliding. *J. Cell Biol.* 63:35–63.

Waxman, L., and A.L. Goldberg. 1982. Protease La from *Escherichia coli* hydrolyzes ATP and proteins in a linked fashion. *Proc. Natl. Acad. Sci. USA.* 79:4883–4887.

Wilkerson, C.G., S.M. King, and G.B. Witman. 1994. Molecular analysis of the γ heavy chain of *Chlamydomonas* flagellar outer arm dynein. *J. Cell Sci.* 107: 497–506.

Witman, G.B. 1986. Isolation of *Chlamydomonas* flagella and flagellar axonemes. *Methods Enzymol.* 134:280–290.

Witman, G., K. Carlson, J. Berliner, and J. Rosenbaum. 1972. *Chlamydomonas* flagella: I. Isolation and electrophoretic analysis of microtubules, matrix, membranes, and mastigonemes. *J. Cell Biol.* 54:507–539.

Witman, G.B., J. Plummer, and G. Sander. 1978. *Chlamydomonas* flagellar mutants lacking radial spokes and central tubules. Structure, composition, and function of specific axonemal components. *J. Cell Biol.* 76:729–747.

Witman, G.B., C.G. Wilkerson, and S.M. King. 1994. The biochemistry, genetics, and molecular biology of flagellar dynein. *In* Microtubules. J.S. Hyams and C.W. Lloyd, editors. Wiley-Liss, New York. 229–250.

Wray, W., T. Boulikas, V.P. Wray, and R. Hancock. 1981. Silver staining of proteins in polyacrylamide gels. *Anal. Biochem.* 118:197–203.